

Structure of $ABi_2Nb_2O_9$ ($A = Sr, Ba$): Refinement of Powder Neutron Diffraction Data

Ismunandar and Brendan J. Kennedy

School of Chemistry, The University of Sydney, New South Wales 2006, Australia

and

Gunawan and Marsongkohadi

Materials Science Research Center, National Atomic Energy Agency of Indonesia, Puspiptek, Serpong, Indonesia

Received March 7, 1996; in revised form July 8, 1996; accepted July 10, 1996

The room temperature structures of the two Aurivillius-type oxides $ABi_2Nb_2O_9$ ($A = Sr, Ba$) have been refined by Rietveld analysis of powder neutron diffraction data. The two oxides are isostructural, with orthorhombic space group $A2_1am$, $Z = 4$, $a = 5.5189(3)$ Å, $b = 5.5154(3)$ Å, $c = 25.1124(9)$ Å for $SrBi_2Nb_2O_9$ and $a = 5.567(1)$ Å, $b = 5.567(1)$ Å, $c = 25.634(1)$ Å for $BaBi_2Nb_2O_9$. Both compounds exhibit a polar and potentially ferroelectric structure. Adoption of perovskite-type layers in the smaller Sr ion containing material results in a tilting of the NbO_6 octahedra, which in turn makes the formation of a fifth strong bond between Bi in the $[Bi_2O_2]^{2+}$ layer and an O from the $[SrNb_2O_7]^{2-}$ layer possible. This bond is absent in $BaBi_2Nb_2O_9$. The formation of the fifth bond in the Sr compound contributes to a larger value of P_s than found in the analogous Ba compound. © 1996 Academic Press, Inc.

INTRODUCTION

In recent years, there has been considerable interest in the ferroelectric Aurivillius compounds, since such materials are widely used in technical devices. Aurivillius-type oxides, which were first reported almost 50 years ago, can be described by the general formula $[M_2O_2]^{2+}[A_{m-1}B_mO_{3m+1}]^{2-}$, where M is usually, but not exclusively, Bi (1). The structures consist of $[Bi_2O_2]^{2+}$ layers interleaved with $(m - 1)$ perovskite-type layers having the composition $[A_{m-1}B_mO_{3m+1}]^{2-}$. Spontaneous polarization in these types of materials can be ascribed both to the displacement of the B cations as well as a tilting of the BO_6 octahedra (2).

The two oxides $ABi_2Nb_2O_9$ ($A = Sr, Ba$) are members of the $[M_2O_2]^{2+}[A_{m-1}B_mO_{3m+1}]^{2-}$ family of compounds with $m = 2$, and were first reported by Aurivillius in 1949 (3), who correctly determined the prototype structure. Shortly

after, the materials were recognized as possible ferroelectrics by Subbarao (4). The Curie temperature, T_c , for these compounds is 420 and 210°C for $A = Sr$ and Ba , respectively. Unlike $SrBi_2Nb_2O_9$, which shows sharp phase transition, $BaBi_2Nb_2O_9$ exhibits a broader temperature dependent phase transition (5). Recent studies on the ferroelectric properties of these compounds showed that these materials have better fatigue endurance than the more widely studied bismuth oxide layer ferroelectric, $Bi_4Ti_3O_{12}$ (6, 7).

In his original work Aurivillius noted an orthorhombic distortion in these types of materials, but failed to observe the weak superstructure reflections and therefore described the structure in an incorrect space group, $Fmmm$. Subsequently, in a study of $(Sr, Ba)Bi_2Ta_2O_9$, Newnham *et al.* proposed that the structure of the material is best described in the orthorhombic space group $A2_1am$ (8). It has been customary to describe the major ferroelectric displacement to be in the a direction. As a result, the Bravais lattice of these types of oxides have almost invariably been reported with an A centering cell. EXAFS studies on the local structure in $Ba_{1-x}Sr_xBi_2Nb_2O_9$ by Wachsmuth *et al.* (2) revealed that the Sr and Ba ions freely substitute for each other, forming an array of solid solutions. Wachsmuth further suggested that differences in the ionic radii of Ba and Sr resulted in significant changes in the tilting and distortion of the surrounding NbO_6 octahedra (2).

To the best of our knowledge there is no report describing the precise crystal structures of $SrBi_2Nb_2O_9$ and $BaBi_2Nb_2O_9$. Therefore, as a part of a wider study of the structural properties of bismuth containing metal oxides (9, 10), we refined the structures of $ABi_2Nb_2O_9$ ($A = Sr,$

TABLE 1
Positional and Thermal Parameters (\AA^2) for $\text{ABi}_2\text{Nb}_2\text{O}_9$
($A = \text{Sr}, \text{Ba}^a$)

$\text{SrBi}_2\text{Nb}_2\text{O}_9$					
$A2_1am$		$R_p = 9.22\%$			
$a = 5.5189(3) \text{\AA}$		$R_{wp} = 11.67\%$			
$b = 5.5154(3) \text{\AA}$		$R_{\text{expt}} = 7.57\%$			
$c = 25.1124(9) \text{\AA}$		$R_{\text{Bragg}} = 4.91\%$			
Atom	Site	x	y	z	B
Sr	4a	0 ^b	0.245(2)	0	0.89(9)
Bi	8b	0.508(3)	0.734(1)	0.2011(2)	1.59(8)
Nb	8b	0.498(3)	0.752(2)	0.4134(1)	0.35(6)
O(1)	4a	0.462(5)	0.211(3)	0	1.7(2)
O(2)	8b	0.470(5)	0.798(2)	0.3410(2)	1.2(1)
O(3)	8b	0.738(3)	-0.005(2)	0.2500(3)	0.89(8)
O(4)	8b	0.673(3)	0.967(2)	0.0849(2)	0.5(1)
O(5)	8b	0.729(3)	0.976(2)	0.5707(2)	0.6(1)
$\text{BaBi}_2\text{Nb}_2\text{O}_9$					
$A2_1am$		$R_p = 9.67\%$			
$a = 5.567(1) \text{\AA}$		$R_{wp} = 12.34\%$			
$b = 5.567(1) \text{\AA}$		$R_{\text{expt}} = 8.16\%$			
$c = 25.634(1) \text{\AA}$		$R_{\text{Bragg}} = 4.39\%$			
Atom	Site	x	y	z	B
Ba	4a	0 ^b	0.275(7)	0	0.9(2)
Bi	8b	0.495(6)	0.753(3)	0.2024(2)	2.9(1)
Nb	8b	0.491(7)	0.754(3)	0.4112(1)	0.34(9)
O(1)	4a	0.464(10)	0.236(6)	0	1.4(2)
O(2)	8b	0.464(8)	0.764(4)	0.3397(2)	1.4(2)
O(3)	8b	0.717(7)	0.000(5)	0.2532(5)	0.29(9)
O(4)	8b	0.723(7)	0.001(6)	0.0785(6)	1.3(3)
O(5)	8b	0.734(7)	0.989(4)	0.5779(5)	0.2(2)

^a Number in parentheses are esd's in the last significant digits.

^b Constrained to be 0.0.

Ba) from powder neutron diffraction data. The results are reported in this paper.

EXPERIMENTAL

$\text{ABi}_2\text{Nb}_2\text{O}_9$ ($A = \text{Sr}, \text{Ba}$) were produced by the solid state reaction of SrCO_3 (Aldrich, 99.5%) or BaCO_3 (Aldrich, 99.98%), Bi_2O_3 (Aldrich, 99.999%), and Nb_2O_5 (Aldrich, 99.9%) at 900°C for 15 h, then at 1000°C for 15 h, and finally at 1200°C for 24 h with regrinding after each heating step. As pointed out by Subbarao (4), this heat treatment eliminates the possibility of incorporation of carbonate in the samples. Preliminary X-ray powder diffraction measurements, carried out on a Siemens D-5000 diffractometer, did not reveal any impurity phases. Scanning electron microscopy (SEM) and energy dispersive X-ray analysis (EDA) were performed on a Phillips SEM 505

equipped with an EDAX PV9900 energy dispersive analyzer.

The neutron powder diffraction patterns were recorded at room temperature using the high-resolution powder diffractometer installed at the neutron guide hall of the G. A. Siwabessy reactor in BATAN (National Atomic Energy Agency of Indonesia). The incident neutron wavelength used was 1.8215 Å from a flat hot pressed Ge(331) single crystal monochromator. A total of 3200 data points were recorded by step scanning at 0.05° interval over the angular range $2.5^\circ < 2\theta < 162.5^\circ$ with 32 He-3 detectors. The lightly ground sample was contained in a thin-walled 16-mm-diameter vanadium can which was slowly rotated during measurement to minimize the effects of preferred orientation.

The Rietveld refinement (11) was undertaken with a PC version of the computer program LHPM (12). The structural parameters reported by Newnham for (Sr, Ba) $\text{Bi}_2\text{Ta}_2\text{O}_9$ (8) were used as a starting model. In the final refinements 44 parameters were varied, including 21 positional parameters and 8 isotropic thermal parameters. The z parameters of A atoms in fourfold equipoint were held constant to establish an origin along the polar axis. The background was defined by fourth-order polynomial in 2θ and was refined simultaneously with the other profile parameters. A Voigt function was chosen to generate the line shape of the diffraction peaks. The Gaussian component has widths given by the function $(\text{FWHM})^2 = U \tan^2 \theta + V \tan \theta + W$ (13), where U , V , and W are refineable parameters and the width of Lorentzian component was varied as $\eta \sec \theta$ to model particle size. The coherent scattering lengths used were $\text{Ba} = 0.525$, $\text{Sr} = 0.702$, $\text{Bi} = 0.8533$, $\text{Nb} = 0.7054$, $\text{O} = 0.580 \text{ fm}$ (10^{-15} m) (14). Attempts to refine structural models in which either Ba or Sr were allowed to occupy the Bi site invariably were unsuccessful. Refinements of the bismuth and oxygen occupancies gave no indication of any deviation from the ideal stoichiometry.

While the refinement on $\text{SrBi}_2\text{Nb}_2\text{O}_9$ proceeded smoothly, the refinement on $\text{BaBi}_2\text{Nb}_2\text{O}_9$ initially did not converge. This is because the displacements from the parent structure in $\text{BaBi}_2\text{Nb}_2\text{O}_9$ are smaller than those in $\text{SrBi}_2\text{Nb}_2\text{O}_9$. For this reason, it was necessary to initially refine positional parameters of one atom at a time, the positional parameters of all other atoms being kept fixed. The procedure was repeated a number of times for all atoms and then finally all 44 parameters were refined simultaneously.

RESULTS AND DISCUSSION

The oxides $\text{ABi}_2\text{Nb}_2\text{O}_9$ ($A = \text{Sr}, \text{Ba}$) were obtained as white polycrystalline powders and exhibited excellent crystallinity as demonstrated in powder XRD patterns.

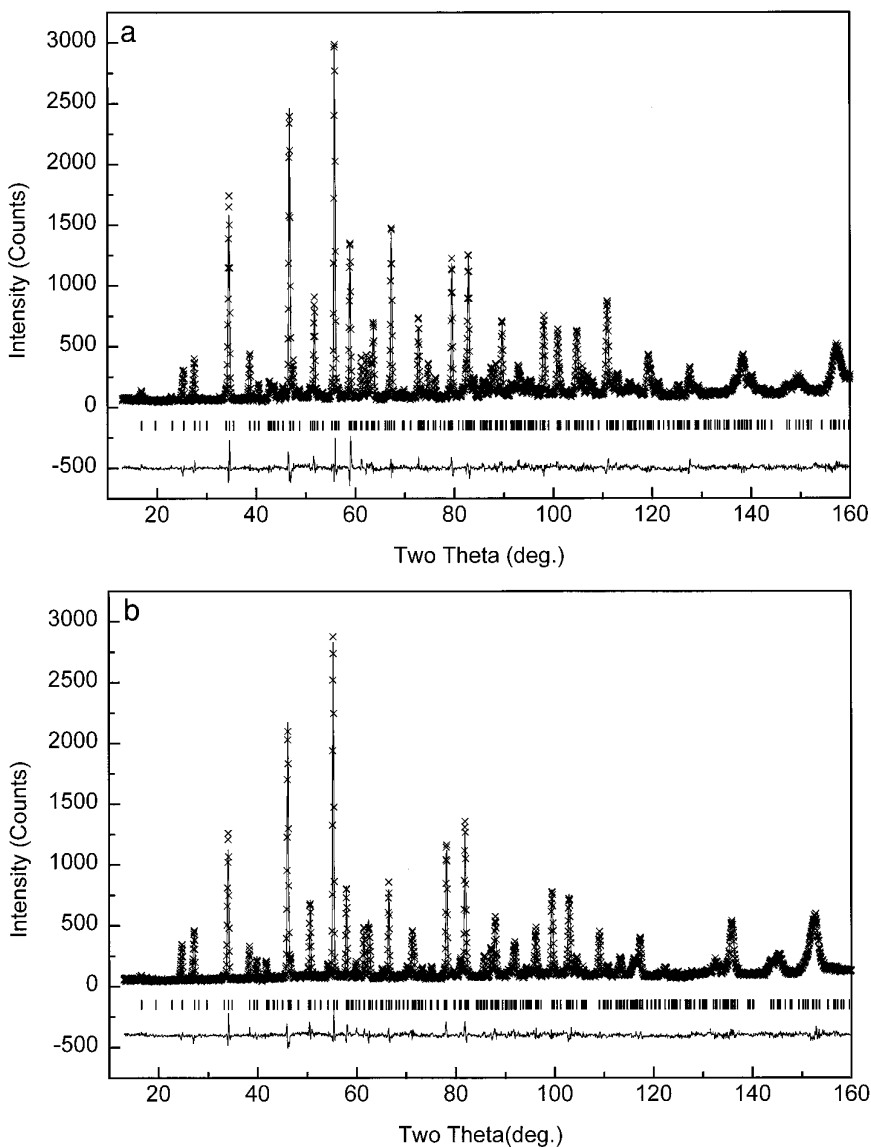


FIG 1. Observed, calculated, and difference neutron powder diffraction profiles for SrBi₂Nb₂O₉ (a) and for BaBi₂Nb₂O₉ (b). The observed profiles are indicated by crosses and the calculated profiles by the solid line. The short vertical lines below the profiles mark the position of all possible Bragg reflections.

The homogeneity of the samples was confirmed by EDA analysis. The final positional parameters, isotropic thermal parameters, and standard R factors for the two oxides are given in Table 1. The agreement between the observed and calculated neutron diffraction profiles are shown in Figs. 1a and 1b. Metal–oxygen bond distances calculated from the final coordinates are presented in Table 2. Oxygen–oxygen distances are not listed, but none were unusual, the shortest being 2.68(4) Å. The metal–oxygen bonds are comparable to those found in related metal oxides and are generally as expected from the sum of the ionic radii of the constituents (15).

The two oxides $ABi_2Nb_2O_9$ ($A = Sr, B$) as members of the $[M_2O_2]^{2+} [A_{m-1}B_mO_{3m+1}]^{2-}$ family of compounds with $m = 2$ consist of $[Bi_2O_2]^{2+}$ layers interleaved with $[ANb_2O_9]^{2-}$ perovskite-type layers. In the prototype structure, Sr or Ba is coordinated to 12 oxygen atoms, bismuth is bonded to 4 oxygen atoms in a square pyramidal geometry, while niobium occupies the MO_6 position in the perovskite layer. The continuous O–Nb–O chains expected in a simple perovskite-type structure are interrupted not only along the c axis by $[Bi_2O_2]^{2+}$ layers but also by translation of the perovskite plane perpendicular to the c axis relative to the neighboring perovskite planes. On the other hand,

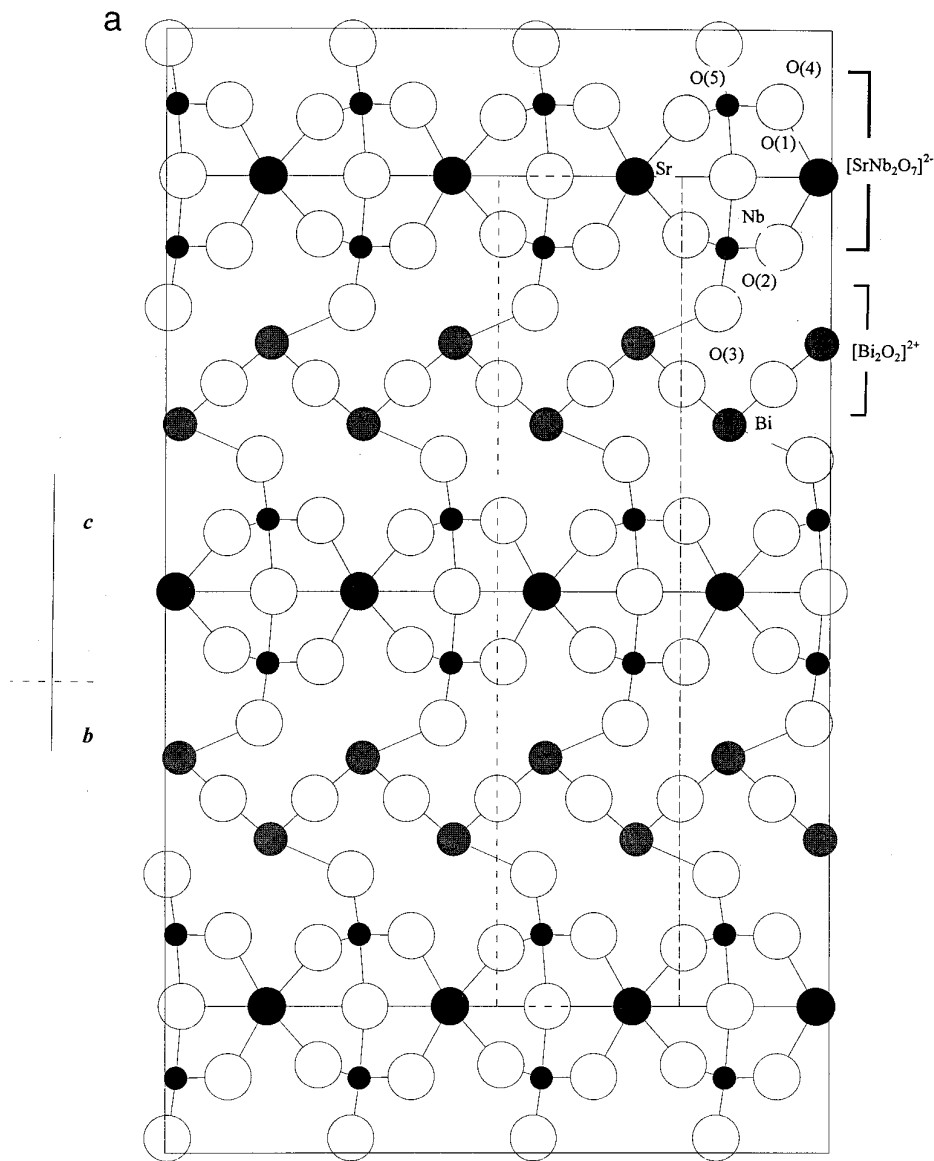


FIG. 2. The (100) projection of $\text{SrBi}_2\text{Nb}_2\text{O}_9$ (a) and $\text{BaBi}_2\text{Nb}_2\text{O}_9$ (b) showing the alternate $[\text{Bi}_2\text{O}_2]^{2+}$ and $[\text{ABi}_2\text{Nb}_2\text{O}_7]^{2-}$ layers. The dashed line represents the unit cell. Note both the displacement of the middle perovskite layers along b relative to the top and bottom layers and the formation of a fifth Bi–O bond in (a).

unbroken O–Nb–O chains are present in the plane perpendicular to the c axis.

In $\text{BaBi}_2\text{Nb}_2\text{O}_9$ the fourfold coordination geometry of Bi atoms is retained (Fig. 2b), while for $\text{SrBi}_2\text{Nb}_2\text{O}_9$ (Fig. 2a), a fifth Bi–O bond to the apex oxygen of the perovskite layer, O(2), is formed. Formation of a fifth bismuth–oxide bond is also observed in $\text{Sr}_{0.9}\text{Ba}_{0.1}\text{Bi}_2\text{Ta}_2\text{O}_9$ (7), $\text{Bi}_2\text{W}_2\text{O}_6$ (16), $\text{Bi}_3\text{Ti}_4\text{O}_{12}$ (17), and $\text{Bi}_3\text{TiNbO}_9$ (18). The general structural features of the $[\text{Bi}_2\text{O}_2]^{2+}$ layer are not altered by replacing Ba with the smaller Sr cations, the average Bi–O distances being 2.4(1) and 2.3(1) Å for $\text{SrBi}_2\text{Nb}_2\text{O}_9$

and $\text{BaBi}_2\text{Nb}_2\text{O}_9$, respectively. In these oxides the Bi–O bonds lie in the range 2.20(2)–2.64(1) Å and are more than 0.20 (4) Å shorter than the nonbonded Bi–O distances. There are 3 (for the Sr compound) and 4 (for the Ba compound) Bi–O distances between 2.80 and 3.52 Å. It should be noted that as a consequence of the $6s^2$ lone pair, distorted Bi geometries are relatively commonplace. For example, in $\text{Bi}_3(\text{MSb}_2)\text{O}_{11}$, ($M = \text{Al}, \text{Ga}$) (10) the two independent bismuth atoms are coordinated to eight and nine O atoms and have three short Bi–O distances of around 2.30 Å, while the remaining Bi–O distances are

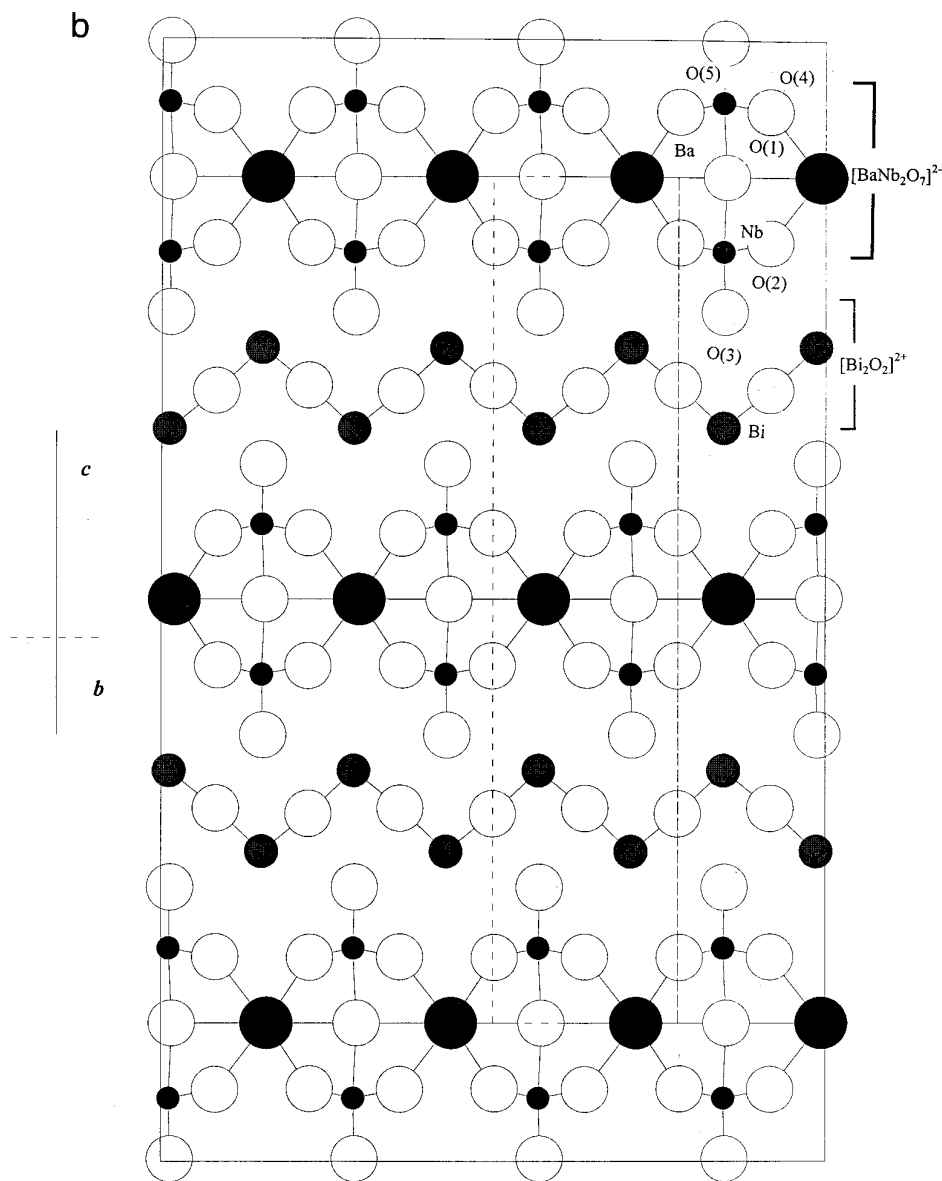


FIG. 2—Continued

about 2.80 Å. The calculated bond valence sums (19) for $SrBi_2Nb_2O_9$ and $BaBi_2Nb_2O_9$ are 2.67 and 2.49, respectively. It appears that in these compounds the bismuth atoms are underbonded.

The thermal parameters of bismuth atoms are unusually high compared to the other, lighter atoms. This can be ascribed to the unusual open geometry of the Bi cations which allows for considerable motion. In $BaBi_2Nb_2O_9$, which has the lower Curie temperature, the Bi atoms are only fourfold coordinated and the Bi thermal parameters are significantly larger than those in $SrBi_2Nb_2O_9$. Attempts to refine anisotropic thermal parameters of the atoms were unsuccessful.

The formation of a fifth Bi–O bond can be explained in terms of the tilting of the NbO_6 octahedra. Stabilization of the perovskite layer, when the smaller Sr^{+2} ion is present, apparently requires the NbO_6 octahedra to tilt by 6° with respect to the c axis. Neighboring octahedra rotate in opposing directions. The role of Sr in promoting this alternation of the tilting appears to be related to the fact that Sr forms one very short bond, 2.53(2) Å, to O(1), the oxygen common to both octahedra in the perovskite layer. This results in a puckered appearance. In addition to this short bond, there are seven other longer bonds that lie between 2.58(2) and 3.18(1) Å. These give rise to an 8-fold geometry coordination, instead of the 12-fold coordination observed

TABLE 2
Bond Distances (Å) for $ABi_2Nb_2O_9$ ($A = Sr, Ba$)^a

		SrBi ₂ Nb ₂ O ₉	BaBi ₂ Nb ₂ O ₉
[Bi ₂ O ₂] ²⁺ layer	Bi–O(2)	2.64(1)	^b
	Bi–O(3)	2.28(1)	2.26(3)
	Bi–O(3)	2.31(1)	2.37(4)
	Bi–O(3)	2.44(1)	2.44(4)
	Bi–O(3)	2.20(1)	2.19(4)
[(Sr, Ba)Nb ₂ O ₇] ²⁻ perovskite layer	(Sr, Ba)–O(1)	2.58(2)	2.59(4)
	(Sr, Ba)–O(1)	2.97(2)	2.84(4)
	(Sr, Ba)–O(1)	3.00(2)	2.99(5)
	(Sr, Ba)–O(1)	2.53(2)	2.73(5)
	(Sr, Ba)–O(4)	3.18(1)	2.96(4)
	(Sr, Ba)–O(4)	2.62(1)	2.82(3)
	(Sr, Ba)–O(5)	2.65(1)	2.76(3)
	(Sr, Ba)–O(5)	2.67(1)	2.72(3)
	Nb–O(1)	2.189(4)	2.284(6)
	Nb–O(2)	1.835(7)	1.837(8)
	Nb–O(4)	2.08(2)	2.08(5)
	Nb–O(4)	1.90(1)	1.93(5)
	Nb–O(5)	2.07(1)	2.04(5)
	Nb–O(5)	1.89(2)	1.90(5)

^a Number in parentheses are esd's in the last significant digits.

^b The corresponding distance is 2.92(3) Å which is best described as a nonbonding contact.

in the prototype structure. In BaBi₂Nb₂O₉, the same degree of tilting of the NbO₆ octahedra is not present presumably as a consequence of the weaker interaction between Ba and O(1). The greater stability of the perovskite layer in BaBi₂Nb₂O₉ is seen in the “tolerance factor”; for [BaNb₂O₇]²⁻ it is 0.87 vs 0.82 for [SrNb₂O₇]²⁻ (20). As a result, the NbO₆ octahedra are tilted by less than 3° with respect to the *c* axis. Although the 8-fold coordination of oxygen to the Ba cation is retained in BaBi₂Nb₂O₉, the relatively small tilting of NbO₆ octahedra results in a more regular Ba–O geometry.

The tilting described above for SrBi₂Nb₂O₉ results in two interesting changes on substitution of Ba for Sr. First, the longest Nb–O(1) bond contracts significantly from 2.284(6) to 2.189(4) Å; contraction of the other Nb–O bonds is much less. Second, the contraction of the *c* parameter is ten times larger than the contraction in the other two directions, which are only marginally reduced on replacement of Ba with Sr. Thus the structural information suggests the Sr compound is much more “strained” than the Ba compound.

In the present work, spontaneous polarizations (P_s) of 31(4) μC cm⁻² and 19(9) μC cm⁻² were calculated for Sr and Ba compounds, respectively (21). While these values are larger than those obtained for SrBi₂Ta₂O₉ and Sr_{1-x}Ba_xBi₂Ta₂O₉ (8, 22), the trend is consistent with the T_c – P_s relationship observed for related compounds (23). The

difference in the calculated P_s between $A = Sr$ and Ba in part is readily identified with the shift in O(2). The formation of the fifth strong bond between Bi and O(2) results in a larger shift in the position of O(2) relative to virtually stationary [001] chains of Bi cations.

In summary, the results of this study show that the distortion of the structure of ABi₂Nb₂O₉ ($A = Sr, Ba$) from the prototype structure occur as consequence of changes in both the bismuth oxide and perovskite layer. This distortion is larger for the compound containing the smaller Sr²⁺ cation. As stated in the Introduction, BaBi₂Nb₂O₉ exhibits a broader thermal evolution of the dielectric constant close to the Curie temperature and Smolenskii suggested that this results from the presence of a Ba²⁺ ion in the Bi site (4). This study, however, does not support this explanation, since there is no evidence that a Bi cation occupies the Ba site. In view of this, further studies on the nature of the phase transition are in progress.

ACKNOWLEDGMENT

We thank PPSM-BATAN for making the facilities available.

REFERENCES

1. B. Aurivillius, *Phys. Rev.* **126**, 893 (1962).
2. B. Wachsmuth, E. Zschech, N. W. Thomas, S. G. Brodie, S. J. Gurman, S. Baker and S. C. Bayliss, *Phys. Status Solidi A* **135**(1), 59 (1993).
3. B. Aurivillius, *Arki. Kemi.* **1**, 463 (1949).
4. E. C. Subbarao, *J. Phys. Chem. Solids* **23**, 665 (1962).
5. G. A. Smolenski, V. A. Isupov and Agranovskaya, *Sov. Phys. Solid State (Engl. Trans.)* **3**, 651 (1959).
6. K. Amanuma, T. Hase and Y. Miyasaka, *Appl. Phys. Lett.* **66**(2), 221 (1995).
7. C. A. Paz de Araujo, J. D. Cuchiaro, M. C. Scott and L. D. McMillan, International Patent Publication No. WO 93/12542 (24 June 1993).
8. R. E. Newnham, R. W. Wolfe, R. S. Horsey, F. A. Diaz-Colon and M. I. Kay, *Mater. Res. Bull.* **8**, 1183 (1973).
9. G. R. Facer, M. M. Elcombe and B. J. Kennedy, *Aust. J. Chem.* **46**, 1897 (1993).
10. Ismunandar, B. J. Kennedy and B. A. Hunter, *J. Solid State Chem.*, submitted for publication.
11. H. M. Rietveld, *J. Appl. Crystallogr.* **2**, 65 (1969).
12. R. J. Hill and C. J. Howard (1986) Australian Atomic Energy Commission Report No. M112, AAEC (now ANSTO), Lucas Heights Research Laboratories, New South Wales, Australia.
13. G. Caglioti, A. Paeloetti and F. P. Ricci, *Nucl. Instrum.* **3**, 223 (1958).
14. V. F. Sears, Atomic Energy of Canada Limited Report AECL-8490, 1984.
15. R. D. Shannon, *Acta Crystallogr.* **32**, 75 (1976).
16. R. W. Wolfe, R. E. Newnham, and M. I. Kay, *Solid State Commun.* **7**, 1797 (1969).
17. J. F. Dorrian, R. E. Newnham, D. K. Smit, and M. I. Kay, *Ferroelectrics* **3**, 17 (1971).
18. R. E. Newnham, R. W. Wolfe and J. F. Dorrian, *Mater. Res. Bull.* **6**, 1029 (1971).
19. N. E. Brese and M. O'Keeffe, *Acta Crystallogr. Sect. B* **47**, 192 (1991).

20. t factors were calculated using the formula $r_A + r_O = t\sqrt{2}(r_{Nb} + r_O)$. The following ionic radii were used Ba^{2+} (CN = 12) = 1.75 Å, Sr^{2+} (CN = 12) = 1.58 Å, Nb^{5+} (CN = 6) = 0.78 Å, and O^{2-} (CN = 6) = 1.26 Å (See (14)).
21. Spontaneous polarization (P_s) was calculated from the equation $P_s = \sum_i (q_i \delta_i) / V$, where q_i and δ_i represent the charge and displacement of i th ions; the summation was made over all I ions in the unit cell with volume V.
22. A. D. Rae, J. G. Thomson, and R. W. Withers, *Acta. Crystallogr. Sect. B* **48**, 418 (1992).
23. K. Singh, D. K. Bopardikar, and D. V. Atkare, *Ferroelectrics* **82**, 55 (1988).